Opto-Electronics Review 28 (2020) 74–81

Opto-Electronics Review

journal homepage: http://journals.pan.pl/opelre

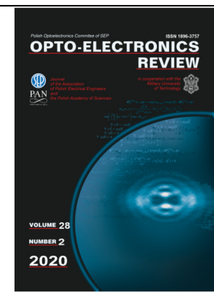

Comparison of photoconductive semiconductor switch parameters with selected switch devices in power systems

K. Piwowarski[a]

[a] Faculty of Electronics, Military University of Technology, 2 gen. Sylwestra Kaliskiego St., Warsaw 00-908, Poland

Article info

Article history:
Received 18 Feb. 2020
Received in revised form 23 Mar. 2020
Accepted 24 mar 2020

Keywords:
electronic devices, electric switch, photoconductive semiconductor switches, gallium phosphide.

Abstract

Currently, work is underway to manufacture and find potential applications for a photoconductive semiconductor switch made of a semi-insulating material. The article analyzes the literature in terms of parameters and possibilities of using PCSS switches, as well as currently used switches in power and pulse power electronic system. The results of laboratory tests for the prototype model of the GaP-based switch were presented and compared with the PCSS switch parameters from the literature. The operating principle, parameters and application of IGBT transistor, thyristor, opto-thyristor, spark gap and power switch were presented and discussed. An analysis of the possibilities of replacing selected elements by the PCSS switch was carried out, taking into account the pros and cons of the compared devices. The possibility of using the currently made PCSS switch from gallium phosphide was also discussed.

1. Introduction

Literature analysis showed that in recent years a growing interest in the use of optical devices both in civil and military systems was observed. The reason for that are their advantages over traditional solutions such as easy control and certainty of switching on moment, and galvanic separation of control and work systems. These features are especially in demand in power and pulse power systems which goal is to deliver high peak power with values of the order of megawatts in short time pulses, often in the order of nanoseconds, with a repetition rate such as 1 kHz. Civilian systems include high voltage pulse generators, such as Marx generator, where they can be used as switches, easier to control and more reliable. They can be also applied in power engineering systems, especially in electrical distribution and transmission. The aim is to improve their reliability, enhance efficiencies, and reduce maintenance and operations costs. Military applications include high frequency antennas, directed energy weapons, pulsed microwave sources, and high-power pulsed lasers, where they are used as system triggers. One of the optical devices meeting the requirements of these systems is a photoconductive semiconductor switch (PCSS).

PCSS is an electrical switch and its operating principle is based on the phenomenon of photoconduction. Excitation of a semiconductor material by a beam of light generates electron-hole pairs which participate in the process of current conduction. Photons in the beam must have energy greater than or equal to the semiconductor bang gap width ($h\nu \geq E_g$) for a direct creation of free charge carriers. In case of a lower photon energy than the band gap width ($h\nu < E_g$) charge carriers are generated through defect centers in material [1]. Photon energy absorption changes semiconductor material conductivity by several orders of magnitude [2] in time of nanoseconds or picoseconds [3] with repetition rates of the order of 1 kHz [4]. In the blocking state, PCSS switches can work at voltages up to 100 kV, while in the conducting state, the flowing current can be as high as 1 kA [4,5] which meets the requirements of the previously discussed systems.

PCSS is usually made of a semiconductor material with a thickness between 0.5 mm to 1.0 mm. On its surface two ohmic contacts are assembled which enables the switch connection to the electrical system. Construction of PCSS switches was discussed in detail in Ref. 6. Figure 1 presents typical constructions and the operation idea of PCSS switches.

* Corresponding author: e-mail karol.piwowarski@wat.edu.pl

https://doi.org/10.24425/opelre.2020.132502
1896-3757 © 2020 Association of Polish Electrical Engineers (SEP) and Polish Academic of Sciences (PAS). Published by PAS.

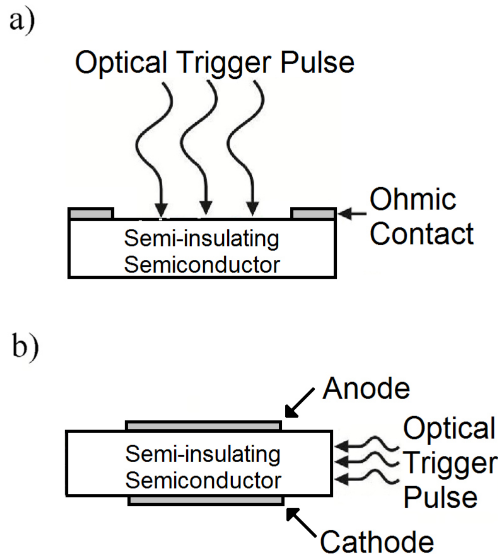

Fig. 1. Construction and operation idea of a PCSS switch: a) lateral geometry and b) vertical geometry.

PCSS characteristics depend on the used semi-insulating (SI) material and its defect structure [7,8]. One of the methods used for studies of deep-level defects in SI materials is the high-resolution photoinduced transient spectroscopy (HRPITS). This method implements correlation and Laplace procedures [9,10]. SI materials currently used to manufacture photoconductive semiconductor switches are InP, GaAs, GaP, 6H-SiC, 4H-SiC, and GaN. These materials are characterized by the band gap energy values at 300 K, equal to 1.34 eV, 1.424 eV, 2.26 eV, 3.0 eV, 3.23 eV, and 3.39 eV, respectively and critical electric field strength values for these materials are equal to 0.5 MV/cm, 0.4 MV/cm, 1.0 MV/cm, 3.0 MV/cm, 3.0 MV/cm, and 5.0 MV/cm [6,11].

Photoconductive semiconductor switches are most often made of SI GaAs. Literature study shows that a semiconductor switch made of SI GaAs can block a voltage up to 40 kV and conduct a current as high as 400 A [5]. During tests it withstands 20 kV blocking voltage and about 350 pulses of a 400 A current in conduction state [4]. Other mentioned SI materials have wider band gaps and, theoretically, should be able to block higher voltages and conduct higher current values than switches made of SI GaAs. Recent studies have experimentally shown that performance of PCSSs made of SI GaP, SI 6H-SiC, SI 4H-SiC, and SI GaN is much better compared to that made of SI GaAs [3,12,13].

PCSS switches can work in two modes: linear, also called conventional, and non-linear, called avalanche. The first one occurs only in low voltage systems which is caused by the fact that activation in linear mode is independent of the electrical field value in the switch. The value of the electric field to which the switch works in this mode depends on the used material. Tests show that in case of SI GaAs it is of around 4 kV/cm. In this mode absorption of one photon generates formation of only one electron-hole pair. After switching off the light source, an excessive charge carriers' recombination occurs, and semiconductor material properties return to the state before illumination. Due to reduced current density, switches operating in linear mode are characterized by a longer lifetime [4].

Avalanche mode depends on electrical field strength in the switch and can only be achieved for higher electric field values than in conventional mode. Specific field strengths' value depends on the material used to manufacture a switch. In this mode excess charge carriers receive additional energy as a result of a strong electric field and impact ionization which occurs by knocking out valence electrons and electrons from defect centers to the conduction band. Because of this a single photon can generate many charge carriers. After initiation, a multiplication process of charge carriers is maintained until the electric field strength in the switch drops below the appropriate value which depends on a semiconductor material. Since the laser beam is used only as a means of triggering the switch, avalanche mode requires lower optical energy than conventional mode [1,14].

Research groups from Military University of Technology and Institute of Electronic Materials Technology made attempt to construct a PCSS switch made of gallium phosphide. Currently, the work is underway to improve and optimize the switch design in order to achieve the highest possible parameters' values such as blocking voltage, conducted current, switching frequency. In this article, a literature analysis was made to assess feasibility of using the PCSS switch in place of other currently used mechanical, electronic and optical switches. For this purpose, the selected switches' parameters were compared to PCSS parameters described in the available literature as well as to the results of measurements for the test sample made of gallium phosphide, which were obtained during the initial research done to manufacture PCSS switches. While comparing the devices, the focus was mainly on the parameters and features such as: operating voltage, conducted current, switching frequency, system control convenience, switching repeatability, and lifetime of the device.

2. GaP PCSS measurements

2.1 Switch sample description

The conducted research is a continuation of the research described in Ref. 15. A test switch made of SI GaP single crystals (SI GaP) constructed in lateral geometry and presented in Fig. 1a), was used in the research. SI GaP plates were in the form of chips with an area of 1 x 1 cm and a thickness of 0.5 mm. Two ohmic contacts were made by applying gold on the polished surface of SI GaP plates. The distance between the contacts, called the switch gap, was of 2 mm. Electrodes made of electrolytic copper were attached to each ohmic contact. Before attaching the electrodes, the material's surface was mechanically and chemically cleaned. Electrodes were made in a form of strips: 0.3 mm thick, 10 mm wide and 15 mm long, with 0.2 mm thick, 2 mm wide and 100 mm long leads. Both electrodes and leads were covered with a silver layer. To ensure protection against external factors and reduce the speed of surface recombination of excess charge carriers, after connecting the electrodes, the switches were coated with a 200 nm SiO_2 layer and, then, embedded in a transparent resin. Figure 2 shows the sample switch ready for testing.

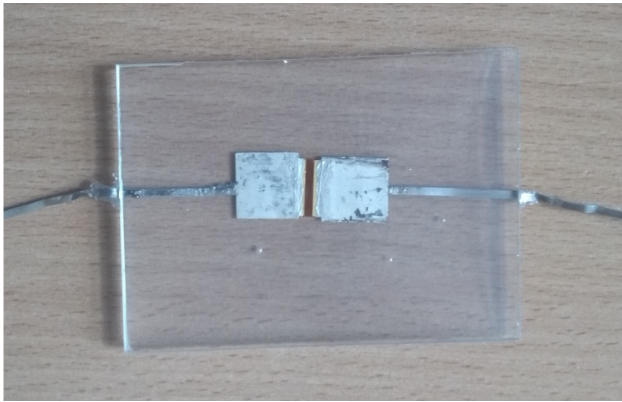

Fig. 2. Sample of PCSS switches made of SI gallium phosphide.

2.2 Dark current measurements

To carry out measurements in blocking state the METREL MI 3210 TeraOhm XA meter was used as a source of DC voltage and as the meter of both current and resistance. It allows for current measurements from 0.1 nA up to 5 nA with a supply voltage in the range of 50 V to 10 kV. Starting from a voltage of 500 V with a step of 500 V, a series of three measurements for each voltage value were made. Obtained results of the resistance dependence from electric field strength are presented in Fig. 3 and the dark current dependence on the voltage in Fig. 4.

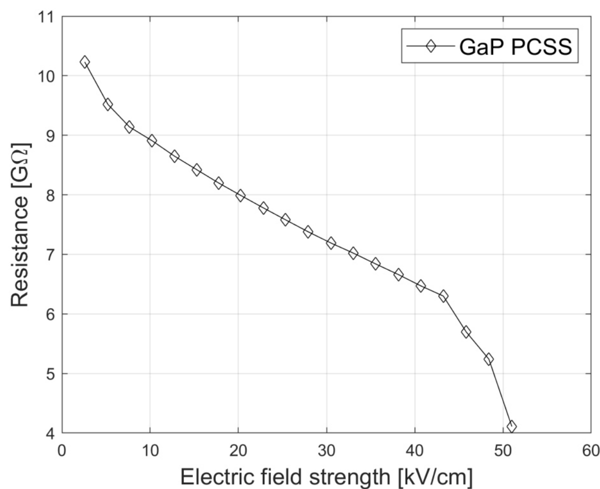

Fig. 3. Dependence of switch resistance on electric field strength in the active area, determined on the basis of dark current intensity measurements at a temperature of 300 K.

Analyzing the characteristics shown in Figs. 3 and 4, it can be seen that in the voltage range from 0.52 kV to 8.65 kV, corresponding to the electric field strength from 2.58 to 43.23 kV/cm, the linear characteristics of the measured PCSS sample were obtained. In the voltage range from 8.65 to 10.2 kV (43.23 to 51 kV/cm) a significant increase in the value of dark current from 1373 to 2480 nA and a decrease in resistance from 6.30 to 4.11 GΩ were

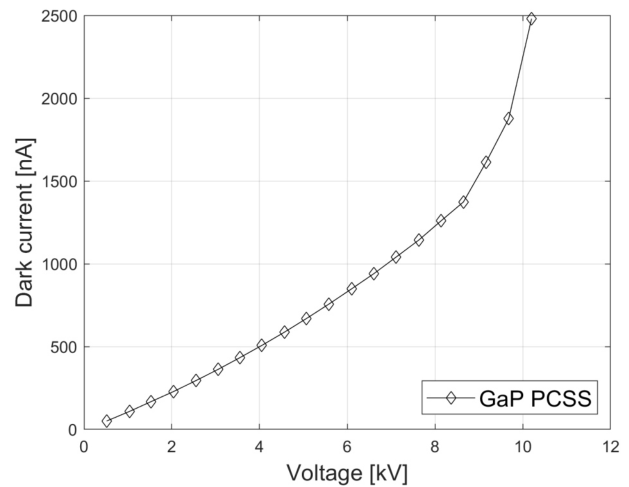

Fig. 4. Current-voltage characteristics of test switch made of SI gallium phosphide measured at 300 K.

observed. The reason for these changes may be a decrease in properties of a transparent resin used to ensure protection against external factors, due to the increase in the operating voltage. As a result, there was an increase in conducted current at the contact surface of SI GaP and resin. Despite the non-linear changes of the measured characteristics for a voltage between 8.65 to 10.2 kV, we can assume that the GaP sample has linear characteristics in blocking state. The blocking resistance in the whole measured range is higher than 1 GΩ, which is acceptable.

2.3 Photocurrent measurements

Measurements in the conduction state were made in a system consisting of the previously mentioned voltage source and connected in series a studied PCSS switch and a 21 MΩ resistor. Voltage drops on the resistor, as well as the system's response to the impulse switching the sample into a conduction state were recorded using an oscilloscope. The photocurrent value was calculated according to Ohm's law for the system discussed and illustrated in Fig. 5.

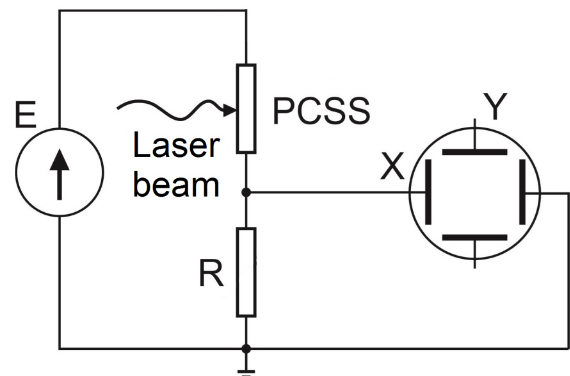

Fig. 5. System diagram used to measure PCSS switch parameters in the conduction state.

The optical switching pulse, with a width of ~ 5 ns, was generated by a tunable laser and the laser beam was emitted with a frequency of 10 Hz. Voltage time courses were recorded after averaging 128 waveforms caused by the optical pulse. The PCSS switch was tested for a wavelength of 710 nm, corresponding to a photon energy of 1.75 eV which is less than a material band gap equal to 2.26 eV with a laser beam energy in the range from 200 to 440 µJ and an applied voltage of 10.2 kV. A specific laser beam length was selected to investigate the effect of laser beam energy on conduction through deep defect centers, thanks to which, after achieving a sufficiently high electric field value, it should allow for the switch to operate in avalanche mode.

Figure 6 shows maximum achieved photocurrent values depending on laser energy. The obtained characteristic is linear which means that the sample switch operates independently of the electric field strength in conventional mode, despite the electric field value of 52 kV/cm. It is much higher than the maximum value for an operation in linear mode obtained for SI GaAs.

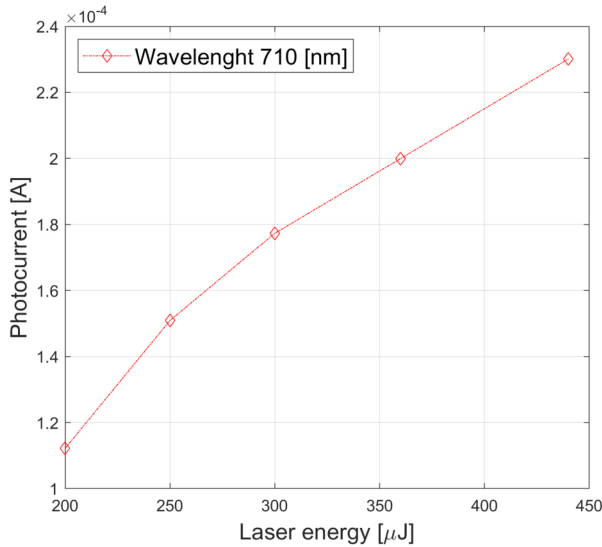

Fig. 6. Maximum photocurrent values of the GaP switch as a function of laser energy, measured at a temperature of 300 K.

Figures 7 and 8 present a photocurrent time course, full and rese period respectively for a laser energy of 440 µJ and an applied voltage of 10.2 kV.

Analyzing the characteristics shown in Figs. 7 and 8, it can be seen that the rise time for the tested GaP switch is much shorter than the fall time about 32 ns and 900 µs, respectively which allows for operating frequency at the level of 1.1 kHz. Relatively long falling time is caused by thermal processes and recombination of carriers through defect centers in a semiconductor material.

Comparing the obtained test results with literature data, it should be noted that the tested switch operates at a much lower blocking voltage and conduct significantly lower current values than presented in the literature. It is necessary to carry out tests at a higher operating voltage of the system and, also, to make effort to increase the value of the conducted photocurrent, since the presented values greatly limit the possibilities of using the tested switch.

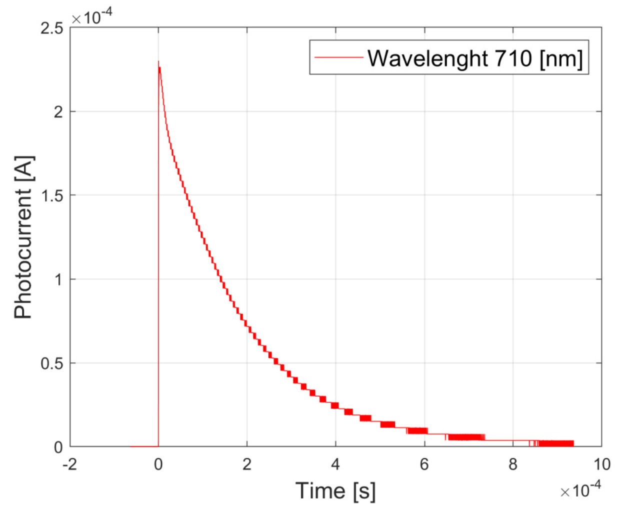

Fig. 7. Full photocurrent time course measured for: laser energy of 440 µJ, wavelenght 710 nm and supply voltage of 10.2 kV at a temperature of 300 K. The moment of switching pulse is at the point t = 0.

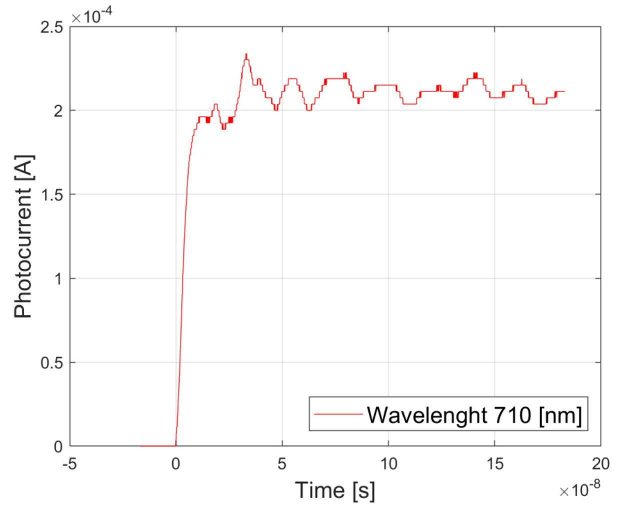

Fig. 8. Rise period of photocurrent time course measured for: laser energy of 440 µJ, wavelenght 710 nm and supply voltage of 10.2 kV at a temperature of 300 K. The moment of switching pulse is at the point t = 0.

3. Competing electrical devices

3.1 IGBT transistor

Insulated-gate bipolar transistor is a semiconductor switching device and is commonly used in uninterruptible power supply units, refrigeration and air conditioning systems, high and medium power inverters and in traction converters [16-18]. This type of transistor consists of MOSFET (Metal-oxide semiconductor field-effect transistor) and BJT (bipolar junction transistor). MOSFET ensures a high impedance gate control and the BJT part provides a low on-state resistance which results in conduction of a high current density. Figure 9 shows a structure of the IGBT transistor.

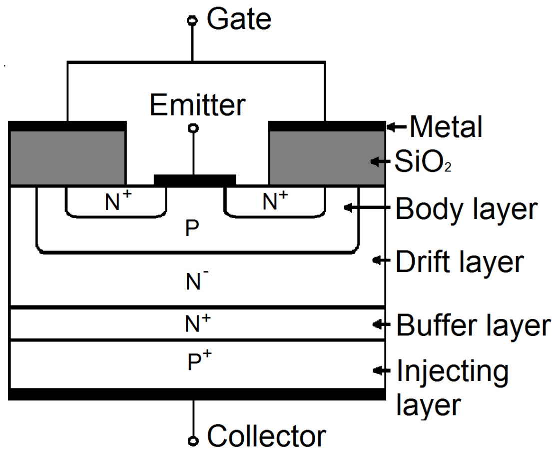

Fig. 9. Structure of the IGBT transistor.

Currently widely available IGBT transistors achieve voltages up to 6.5 kV and can conduct currents up to 2000 A with a switching frequency of 10 kHz [19]. Studied in recent years high frequency IGBT transistors achieved a switching frequency up to 100 kHz at the expense of a significantly lower work voltage and conducted current values of 1200 V and 800 A, respectively [20]. Comparing it with PCSS parameters, IGBT transistors can achieve switching frequency over 10 times higher than PCSS switches and similar values of conducted currents in on-state. Both devices have a compacted structure. PCSS switches can withstand voltages about 15 times higher and provide galvanic separation of the control and operation system.

Based on the collected information, it can be stated that PCSS should be better suited for application in high voltage and power pulse systems which do not require switching frequency higher than 1 kHz as IGBT transistors.

3.2 *Thyristor*

Thyristors are semiconductor devices used in a high current or high voltage signal switching. The thyristor consists of four alternately arranged semiconductor layers forming three p-n junctions in the form of a p-n-p-n structure. They have three leads called anode, cathode and gate. Anode lead is connected to the first p-type layer (P_1) and cathode is connected to the second n-type layer (N_1). The gate lead provides a more convenient control possibility. It can be said that the thyristor consists of two connected bipolar transistors type P_1-N_1-P_2 and N_1-P_2-N_2 in such a way that their emitters are connected to the anode and cathode, while their collectors are the bases of opposite transistors. Figure 10 b) shows a thyristor p-n-p-n structure and as a connection of two bipolar transistors.

These devices can be switched on by supplying a sufficiently high current to the anode or by applying a short current pulse to the gate, after which the conduction state is maintained automatically. Currently widely available thyristors achieve blocking voltages up to 10 kV and currents up to 5 kA [21-23] with the switching frequency up to 10 kHz. Length, height and width of these devices usually do not exceed 5 cm [24].

Based on the information provided PCSS switches can theoretically replace thyristors in high voltage switching systems such as voltage multipliers and in systems where separation of work and control systems is important.

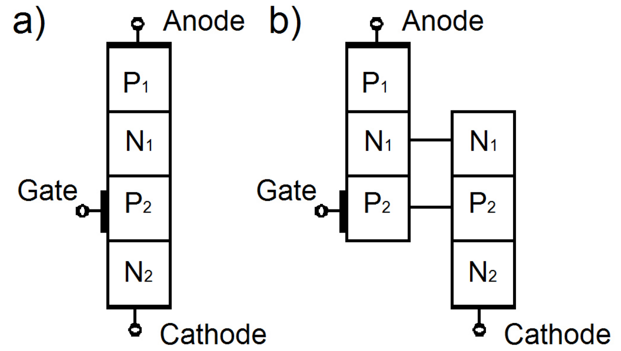

Fig. 10. Thyristor construction: a) layer structure, b) in the form of two connected bipolar transistors.

3.3 *Opto-thyristors*

Opto-thyristor is an optical semiconductor device, typically used as a switching element in high voltage electronic systems. They can be switched on in the same way as the thyristors described in the previous chapter, but the gate is controlled by a light beam achieved usually through a light-emitting diode (LED) or a laser. Thanks to which they have an advantage of the possible galvanic separation between the control and operation systems. Figure 11 shows the construction of the opto-thyristor.

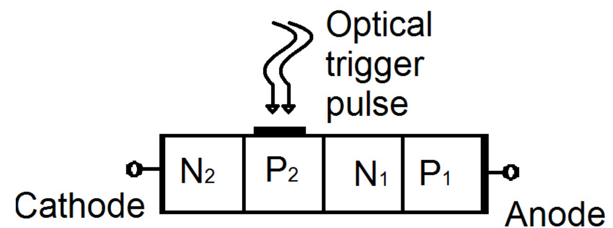

Fig. 11. Construction of the opto-thyristor.

A single dimension of these devices usually does not exceed 2 cm [25]. Commercially available opto-thyristors usually can block voltages in the range of 0.8 to 10 kV and conduct currents between 20 A to 5 kA [26-28]. The switching frequency of these devices is in the range from 1 kHz to 1 MHz [29].

Based on collected data, PCSS switch can be used instead of opto-thyristors in high power and voltage pulse systems where the higher values of blocking voltage are necessary.

3.4 *Spark gap*

Spark gap is an electrical device consisting of two electrodes with a gap between them which is filled with selected liquid, vacuum or pressured gas such as SF_6 and N_2 [30]. Figure 12 shows a spark gap with cone shape electrodes. The air insulation used there is regulated by the distance between the electrodes. Dielectric strength of dry air under normal conditions is about 30 kV/cm.

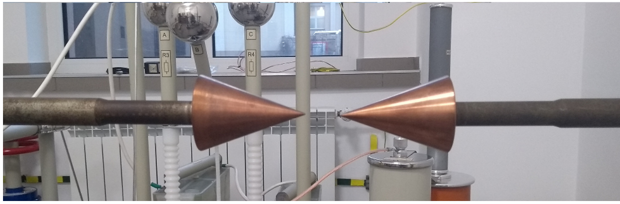

Fig. 12. Image of the spark gap with cone shape electrodes.

Spark gap switches are often used in a pulse power application such as lasers and Marx generators. It has a simple operation principle. When the potential difference between two electrodes exceeds breakdown voltage of a given medium, a spark is formed which ionizes the medium and significantly reduces its resistance, creating a current flow path. When the potential difference between electrodes decreases, the medium stops ionization and the spark extinguishes. Due to the fact, that these devices are used in voltage multipliers, it can be said that the maximum voltage is limited only by the strength of the electrode material. Currently manufactured spark gaps can operate at voltages up to 150 kV and conduct currents up to 100 kA with an operating frequency of up to 1 kHz. Devices that work with frequencies up to 1 MHz are tested, however, these models operate at much lower values of conducted current, within 1 kA [31].

Since the spark gap lifetime decreases with the electrode distance and the breakdown voltage is limited by properties of the used medium, in order to increase it without decreasing overall lifetime, the spark gap is usually placed in a sealed housing under pressure due to which the whole structure significantly expands. The rise time of this switch is measured in nanoseconds, but the exact moment of switching cannot be controlled [32-34].

Based on collected information PCSS switch can replace spark gap switched in systems where it is important to control the exact moment of switching and where a compact switch design is recommended.

3.5 Power switch

Power switch is a mechanical device commonly used in distribution and transmission of electrical energy in high and medium power networks. This switch consists of two electrical contacts, typically one stationary and one movable, where current flows after both contacts touch.

Currently manufactured power switches can operate at a voltage up to 500 kV. The operating current can reach a value up to several kA and at the very moment of switching on, it can exceed 100 kA. The typical frequency is in the order of 50 Hz. Specific problems to that type of a switch are the following: switching time spread, process of contacts recoil during switching on and risk of an electric arc when switching the switch on and off [35,36]. In order to prevent the formation of an electric arc, this type of switch often has arc extinguish chambers. Figure 13 shows an example of the design of power switches with arc extinguishing chambers.

Based on the information provided, PCSS switch can be good alternative for power switch in systems requiring higher operating frequency and where compact switch design is advisable. The use of a PCSS switch together with

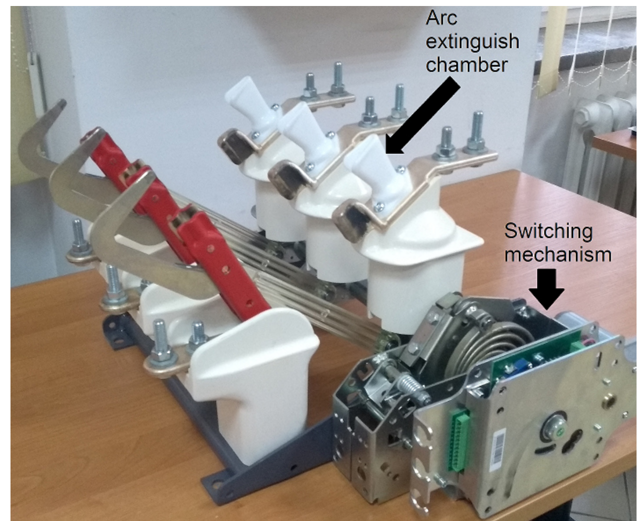

Fig. 13. Image of the power switch with arc extinguishing chambers and mechanical switching mechanism. The rated voltage of the device is of 62 kV.

a power switch in a hybrid switch may eliminate power switch disadvantages while maintaining the ability to work at high voltages [37].

4. Conclusions

The article analyzes the available literature on parameters and possibilities of the PCSS switch application. Results of our research on PCSS switches made of gallium phosphide are presented. Mechanical, electronic and optoelectronic switches were described, as well as a review of their current applications and obtained parameters. An analysis of the possibility of replacing these elements with PCSS switches was also carried out.

Photoconductive semiconductor switches possess many positive features compared to currently used switches. They achieve higher voltage values in the blocking state compared to IGBTs, thyristors, opto-thristors and opto-triacs, as well as higher values of conducted current in relation to opto-thyristors and opto-triacs. They work at a higher frequency than thyristors and power switches. They provide good control of switching on time and compact construction in comparison to spark gaps and power switches. Their advantage, which only other optoelectronic elements, such as opto-thyristors and opto-triacs possess is galvanic separation of the control and operation system. The analysis shows that it is possible to widely use a PCSS switch technology in high voltage and power pulse systems, as well as in electricity transmission and distribution systems.

The tested switch made of gallium phosphide in blocking state withstands a voltage up to 10.2 kV with a dark current value of 2.5 µA. In conduction state for a voltage of 10.2 kV a conducted current of 234 µA was reached which is more than 90 times higher than in blocking state. The rise time was of about 30 ns, but a long fall time of 900 µs limits the possible operating frequency to 1.1 kHz. Still, the rise time in order of nanoseconds and operating frequency at kHz level provide satisfactory results for the prototype, in line with expectations.

At this time, the manufactured and tested switch can only be used in high voltage pulse systems, such as the Marx generator for the first stage of voltage multiplication. They can provide a better control of the switching moment than commonly used spark gaps.

Aim of the further research will be to increase blocking voltage and current in conduction state, as well as to test the switch with vertical geometry.

References

[1] Wolfe T. S. *et al.,* Integrated Computational Investigation of Photoconductive Semiconductor Switches in Pulsed Power Radio Frequency Applications, *IEEE Transactions on Plasma Science*, **44,** 60-70 (2016). https://doi.org/10.1109/TPS.2015.2500022

[2] Mazumder. S. K., An Overview of Photonic Power Electronic Devices, *IEEE Transactions on Power Electronics*, **31,** 6562-6574 (2016). https://doi.org/10.1109/TPEL.2015.2500903.

[3] Xu, M., Liu, X., Li, M., Liu, K., Qu, G., Wang, V., Hu, L. & Schneider, H. Transient characteristic of interdigitated GaAs photoconductive semiconductor switch at 1-kHz excitation. *IEEE Electron Device Letters* **40,** 1136-1138 (2019). https://doi.org/10.1109/LED.2019.2916427

[4] Tian, L. & Shi, W. Analysis and operation mechanism of semi-insulating GaAs photoconductive semiconductor switches. *J. Appl. Phys*. **103**, 124512-1-7 (2008). https://doi.org/10.1063/1.2940728.

[5] Shi, W., Tian, L., Liu, Z., Zhang, L., Zhang, Z., Zhou, L., Liu, H. & Xie, W. 30 kV and 3 kA semi-insulating GaAs photoconductive semiconductor switch. *Appl. Phys. Lett*. **92**, 043511-1-3 (2008). https://doi.org/10.1063/1.2838743.

[6] Majda-Zdancewicz, E., Suproniuk M., Pawłowski, M. & Wierzbowski, M. Current state of photoconductive semiconductor switch engineering. *Opto-Electron. Rev.* **26**, 92-102 (2018). https://doi.org/10.1016/j.opelre.2018.02.003.

[7] Suproniuk M., Kamiński P., Kozłowski R. & Pawłowski M. Efect of deep-level defects on transient photoconductivity of semi-insulating 4H-SiC. *Acta Physica Polonica A* **125,** 1042-1048 (2014). https://doi.org/10.12693/APhysPolA.125.1042

[8] Suproniuk M., Kamiński P., Pawłowski M., Kozłowski R. & Pawłowski M. An intelligent measurement system for the characterisation of defect centres in semi-insulating materials. *Przeglad Elektrotechniczny* **86,** 247-252 (2010). In Polish: [Baza wiedzy w inteligentnym systemie pomiarowym do badania centrów defektowych w półprzewodnikowych materiałach półizolujących]

[9] Suproniuk, M., Pawłowski, M., Wierzbowski, M., Majda-Zdancewicz, E. & Pawłowski, M. K. Comparison of methods applied in photoinduced transient spectroscopy to determining the defect center parameters: The correlation procedure and the signal analysis based on inverse Laplace transformation. *Review of Scientific Instruments* **89**, 04470-0044710 (2018). https://doi.org/10.1063/1.5004098.

[10] Suproniuk, M., Kamiński, P., Kozłowski, R., Pawłowski, M. & Wierzbowski, M., Current status of modelling the semi-insulating 4H–SiC transient photoconductivity for application to photoconductive switches. *Opto-Electron. Rev.* **25**, 171-180 (2017). https://doi.org/10.1016/j.opelre.2017.03.006

[11] Kelkar, K. S., Islam, N. E,. Fessler C. M. and Nunnally W. C., Design and characterization of silicon carbide photoconductive switches for high-field applications, *J. Appl. Phys*., **100**, 124205-1-5 (2006). https://doi.org/10.1063/1.2365713

[12] Luan, C., Feng, Y., Huang, Y., Li, H., Li, X., Research on a novel high-power semi-insulating GaAs photoconductive semiconductor switch, *IEEE Transactions on Plasma Science*, **44,** 5, 839-841 (2016). https://doi.org/10.1109/TPS.2016.2540161

[13] Mauch, D., Sullivan, W., Bullick, A., Neuber, A. & Dickens, J. High Power Lateral Silicon Carbide Photoconductive Semiconductor Switches and Investigation of Degradation Mechanisms. *IEEE Transactions on Plasma Science* **43,** 2021-2031 (2015). https://doi.org/10.1109/TPS.2015.2424154

[14] Long, H., Jiancang, S., Zhenjie, D., Qingsong H. & Xuelin, Y. Investigation on properties of ultrafast switching in a bulk gallium arsenide avalanche semiconductor switch. *J. Appl. Phys*. **115**, 094503-1-7 (2014). https://doi.org/10.1063/1.4866715

[15] Suproniuk M., Kamiński, P., Kozłowski, R., Teodorczyk, M., Mirowska, A., Majda-Zdancewicz, E., Wierzbowski, M., Piwowarski, K. & Paziewski, P. Semi-insulating GaP as a material for manufacturing photoconductive semiconductor switches. *Proc. SPIE* **11055**, (2019). https://doi.org/10.1117/12.2524108

[16] Castagno S. & Curry R D. Analysis and Comparison of a Fast Turn-On Series IGBT Stack and High-Voltage-Rated Commercial IGBTS. *IEEE Transactions on Plasma Science*, **34,** 1692-1696 (2006). https://doi.org/10.1109/TPS.2006.879551

[17] Huang X., Chang W. & Zheng T. Q. Study of the Protection and Driving Characteristics for High Voltage High Power IGBT Modules Used in Traction Convertor. *IEEE 10th Conference on Industrial Electronics and Applications* (ICIEA), (2015) https://doi.org/10.1109/ICIEA.2015.7334314

[18] Ravikumar A. R., *et al.* Uninterruptible power supply employing IGBTs in parallel with electronic protection. *Proceedings of International Conference on Power Electronics, Drives and Energy Systems for Industrial Growth,* (1996). https://doi.org/10.1109/PEDES.1996.536409

[19] Zhang L., Sun K., Huang L. & Igarashi S. Comparison of RB-IGBT and normal IGBT in T-type three-level inverter. in *15th European Conference on Power Electronics and Applications (EPE)*, (2013). https://doi.org/10.1109/EPE.2013.6631823

[20] Schwarzer U. *et al*. Design and Implementation of a Driver Board for a High Power and High Frequency IGBT Inverter. *IEEE 33rd Annual IEEE Power Electronics Specialists Conference. Proceedings (Cat. No.02CH37289)*, (2002). https://doi.org/10.1109/PSEC.2002.1023092

[21] Xu X. *et al*. High-Voltage 4H-SiC GTO Thyristor with Multiple Floating Zone Junction Termination Extension. in *1st Workshop on Wide Bandgap Power Devices and Applications in Asia (WiPDA Asia),* (2018). https://doi.org/10.1109/WiPDAAsia.2018.8734630

[22] Sujod M. Z. 6 Pulse GTO Thyristor Converter Simulation. in *5th Student Conference on Research and Development*, (2007). https://doi.org/10.1109/SCORED.2007.4451395

[23] Ibuka S., Yamamoto A., Hironaka Y., Osada T., Yasuoka K., Ishii S. & Shimizu N. Evaluation of 5500 V-class SI-thyristor as pulsed power switching device utilizing a low inductance testing circuit. in *Conference Record of the Twenty-Third International Power Modulator Symposium (Cat. No. 98CH36133)*, (1998). https://doi.org/10.1109/MODSYM.1998.741204

[24] Rishi N., Ponmurugavel P. S. & Kumar R. D. Attempt To Replace Spark Gap By Thyristor In Marx Circuit, in *International Conference on Power, Energy and Control (ICPEC),* (2013). https://doi.org/10.1109/ICPEC.2013.6527655

[25] Hur J. H., *et al*. GaAs-Based Opto-Thyristor for Pulsed Power Applications. *IEEE Transaction on Electron Devices*, **37,** 2520 – 2525, (1990). https://doi.org/10.1109/IEDM.1989.74307

[26] Schulze H.-J., Niedernostheide F.-J., Kellner-Wedehausen U. & Scheider C. Experimental and numerical investigations of 13-kV diodes and asymmetric light-triggered thyristors, in *European Conference on Power Electronics and Applications*, (2005). https://doi.org/10.1109/EPE.2005.219296

[27] Wang X., *et al.* 4H-SiC Light Triggered Thyristor with Gradually Doped Thin n-base, in *1st Workshop on Wide Bandgap Power Devices and Applications in Asia (WiPDA Asia*), (2018). https://doi.org/10.1109/WiPDAAsia.2018.8734565

[28] Flores D., Hidalgo S., Villamor A., Mcquaid S. & Mazarredo I. Improving the firing mechanisms in thyristors for lighting applications. *Proceedings of the 8th Spanish Conference on Electron Devices (CDE'2011),* (2011). https://doi.org/10.1109/SCED.2011.5744182

[29] Lis R. J., *et al*. An LPE Grown InP Based Optothyristor for Power Switching Applications*, IEEE Transaction on Electron Devices*, **41,** 809 – 813 (1994). https://doi.org/10.1109/16.285035

[30] Arsić N., Osmoković P., Jevtovic B. & Kostic D. The influence of the gas insulation parameters on the triggered three-electrode spark gap functioning. in *IEEE Annual Report Conference on Electrical Insulation and Dielectric Phenomena*, (1997). https://doi.org/10.1109/CEIDP.1997.641137

[31] Lee B-J., Rahaman H., Frank K. & Nam S. H. High Repetitive Switching of Parallel Micro-Plasma Spark Gaps, in *19th IEEE Pulsed Power Conference (PPC)*, (2013). https://doi.org/10.1109/PPC.2013.6627572

[32] Kurhade R. I.,et. al., Implementation of Fast Trigger Generator for High Coulomb Spark Gap Switching, in *3rd International*

Conference on Advances in Electrical, Electronics, Information, Communication and Bio-Informatics (AEEICB17), (2017). https://doi.org/10.1109/AEEICB.2017.7972319

[33] Rahaman H., *et al*, Investigation of Spark Gap Discharge in a Regime of Very High Repetitition Rate. *IEEE Transactions on Plasma Science*, **38,** 2752–2757 (2010). https://doi.org/10.1109/TPS.2010.2052368

[34] Kumar R., *et al.* Development of Synchronization system of Two Spark Gaps, in *IEEE 5th India International Conference on Power Electronics (IICPE)*, (2012). https://doi.org/10.1109/IICPE.2012.6450455

[35] Berczyński, R., & Kulas, S. J. Analysis of the movement dynamics of contacts and contact-set of the making switches. *Przegląd Elektrotechniczny* **93,** 16 - 20 (2017). In Polish: [Badanie dynamiki ruchu styków załącznika zwarciowego] https://doi.org/10.15199/48.2017.10.04

[36] Kulas, S.J. The problems of calculation the arc switching time in tulip contact switches. *Proceedings of the 50th IEEE Holm Conference on Electrical Contacts and the 22nd International Conference on Electrical Contacts Electrical Contacts*, (2004). https://doi.org/10.1109/HOLM.2004.1353153

[37] Kulas S.J., Suronowicz H., Suproniuk M. & Michta, K. Conception a single – phase hybrid switch for power applications, *Przeglad Elektrotechniczny*, **92,** 37–40 (2016). In Polish: [Koncepcja jednofazowego łącznika hybrydowego do zastosowań energetycznych] https://doi.org/10.15199/48.2016.01.